Antitumor Agents

International Edition: DOI: 10.1002/anie.201605892
German Edition: DOI: 10.1002/ange.201605892

Well-Defined Polymer–Paclitaxel Prodrugs by a Grafting-from-Drug Approach

*Benoit Louage, Lutz Nuhn, Martijn D. P. Risseeuw, Nane Vanparijs, Ruben De Coen, Izet Karalic, Serge Van Calenbergh, and Bruno G. De Geest**

Abstract: *We report on the design of a polymeric prodrug of the anticancer agent paclitaxel (PTX) by a grafting-from-drug approach. A chain transfer agent for reversible addition fragmentation chain transfer (RAFT) polymerization was efficiently and regioselectively linked to the C2′ position of paclitaxel, which is crucial for its bioactivity. Subsequent RAFT polymerization of a hydrophilic monomer yielded well-defined paclitaxel–polymer conjugates with high drug loading, water solubility, and stability. The versatility of this approach was further demonstrated by ω-end post-functionalization with a fluorescent tracer. In vitro experiments showed that these conjugates are readily taken up into endosomes where native PTX is efficiently cleaved off and then reaches its subcellular target. This was confirmed by the cytotoxicity profile of the conjugate, which matches those of commercial PTX formulations based on mere physical encapsulation.*

Cancer remains a leading cause of death, and the high incidence of side effects caused by chemotherapeutics urges the development of novel, more efficient formulations for such drug molecules. Paclitaxel (PTX) ranks amongst the most potent and widely used drugs for anticancer treatment; its mechanism of action entails binding tubulin, thereby stabilizing microtubules and preventing their depolymerization. The latter arrests dividing cells at the G2/M phase and eventually leads to apoptotic cell death.[1] PTX has a very low water solubility, and Taxol, the first PTX formulation approved for clinical use, contains the surfactant cremophor EL, which by itself is also prone to cause side effects. Extensive research endeavors have been devoted to the formulation of PTX into alternative nanoparticulate formulations based on non-toxic surfactants, such as albumin (e.g., Abraxane), or amphiphilic block copolymers (e.g., Genexol-PM).[2–5] The latter two commercial formulations have proven to reduce side effects and allow for higher PTX dosing.[6,7] Though considered as nanoformulations, both do not show significant differences in pharmacokinetics compared to free PTX.[8] Previous studies suggest that this is due to fast systemic PTX release from the nanoparticles by passive diffusion and subsequent adsorption to plasma proteins such as endogenous human serum albumin (HSA), thereby annihilating controlled drug release.[9]

Chemical conjugation of PTX might offer a promising solution to limit burst release effects. This strategy not only prevents abrupt systemic toxicity, but can also confer longer blood circulation and increase tumor accumulation by the EPR effect.

In this regard, drug–polymer conjugates have witnessed intensive development since they were introduced by Ringsdorf in the 1970s.[10] A popular ligation strategy involves linking a hydrophilic polymer to PTX through esterification of the hydroxy moieties of the drug. Several such PTX–polymer conjugates have been obtained by post-polymerization modification of preformed polymers with PTX at their backbone or chain end.[11] Such grafting-onto approaches, however, suffer from similar limitations as witnessed in the polymer–protein conjugation field,[12,13] including steric hindrance, which leads to poor conjugation efficiencies, difficulties to control and assess site specificity, and cumbersome purification challenges to remove non-reacted polymer and drug. With respect to the alternative use of drug-linked monomers, issues can arise from the formation of very hydrophobic pockets at high drug loadings, which results in very slow drug release owing to limited water access. Furthermore, as drug conjugation is typically done by ester, hydrazone, or ketal formation, the resulting polymeric degradation products are polyanionic or polycationic or contain polyhydrazines/polyhydrazides or polyaldehydes/polyketones. These polymeric species hold toxicity risks, including long-term accumulation in the body.

Therefore, alternative synthetic techniques are required for designing well-defined polymeric prodrugs with reduced heterogeneity that combine high drug loading with high water solubility and the possibility to introduce additional functionalities. An emerging strategy to address this issue is grafting-from-drug polymerization, an approach that has also gained interest in the polymer–protein conjugation field.[14–19] With the advent of controlled polymerization methods, this strategy yields access to well-defined drug–polymer conjugates with good control over the polymer length and one drug molecule per polymer chain, and, importantly, allows for simple purification, that is, removal of residual monomers. Ring-opening polymerization of lactide from PTX towards polylactide was reported[20] to yield well-defined, but hydrophobic, polymeric prodrugs that required additional surfactants to obtain a stable formulation in aqueous medium.

[*] B. Louage, Dr. L. Nuhn, N. Vanparijs, R. De Coen, Prof. Dr. B. G. De Geest
Biopharmaceutical Technology Unit
Department of Pharmaceutics
Ghent University, Ghent (Belgium)
E-mail: br.degeest@ugent.be
Dr. M. D. P. Risseeuw, I. Karalic, Prof. Dr. S. Van Calenbergh
Laboratory of Medicinal Chemistry
Department of Pharmaceutics
Ghent University, Ghent (Belgium)

Supporting information for this article can be found under: http://dx.doi.org/10.1002/anie.201605892.

Nicolas and co-workers have reported on the preparation of hydrophobic nanoparticles by RAFT- and NMP-mediated polymerization of squalene methacrylate from another drug molecule, gemcitabine, which was covalently modified with a RAFT chain transfer agent or NMP initiator.[21]

Herein, we report on the regioselective synthesis of amphiphilic PTX–polymer conjugates by RAFT polymerization using a PTX-ligated chain transfer agent (CTA), in which PTX and the polymer chain serve as the hydrophobic and hydrophilic segments, respectively. To highlight the versatility of this approach, we also demonstrate the possibility for post-polymerization modification of the opposite polymer chain end. This was exemplified for the attachment of a fluorescent tracer molecule, but small-molecule cancer-cell-targeting ligands could also be used. Our synthesis strategy is depicted in Scheme 1 and begins with the direct ligation of a RAFT CTA (2-(butylthiocarbonothioylthio)propanoic acid (PABTC)) to the C2′ hydroxy group of PTX, which possesses the highest reactivity for esterification.[22] After purification by flash column chromatography, the PTX–RAFT CTA (PTX–PABTC) was obtained in high yield (93 %) and high purity as confirmed by NMR spectroscopy and mass spectrometry (ESI-MS; Figure 1; see also the Supporting Information, Figures S10–S15). In the ^{1}H NMR spectra, the resonances for both PTX and PATBC were found and integrated with excellent correlation. Regioselective modification at the C2′ position of PTX was confirmed by the disappearance of the C2′ OH proton at 3.85 ppm (d, J = 5.5 Hz, 1H) aside from a shift of resonance of the adjacent C2′ proton from 4.77 ppm (dd, J = 5.5, 2.8 Hz, 1H) to 5.45 ppm (dd, J = 12.9, 2.6 Hz, 1H). As the C2′ hydroxy group is crucial for the bioactivity of PTX,[23] an inactive polymeric prodrug was obtained. Subsequently, PTX–PABTC was used for RAFT polymerization of *N*,*N*-dimethylacrylamide (DMA). PolyDMA is a hydrophilic and biocompatible polymer,[24] but other vinyl monomers can also be used as long as they are soluble in an organic solvent in which a PTX-functionalized RAFT CTA can be dissolved. A moderate degree of polymerization (DP) of 30 DMA repeating units was targeted to obtain a conjugate with both high water solubility and PTX loading. Furthermore, a PTX–polyDMA conjugate with a DP of 15 was prepared with PTX–PABTC and a PTX-free polymer with PABTC with a DP of 30. Triple precipitation from ether, in which both CTAs as well as free PTX are soluble but polyDMA and PTX–polyDMA are not, led to isolation of the pure PTX–polymer conjugates and the control polymer. Size exclusion chromatography (SEC; Figure 2 A) revealed the formation of polymers with a narrow weight

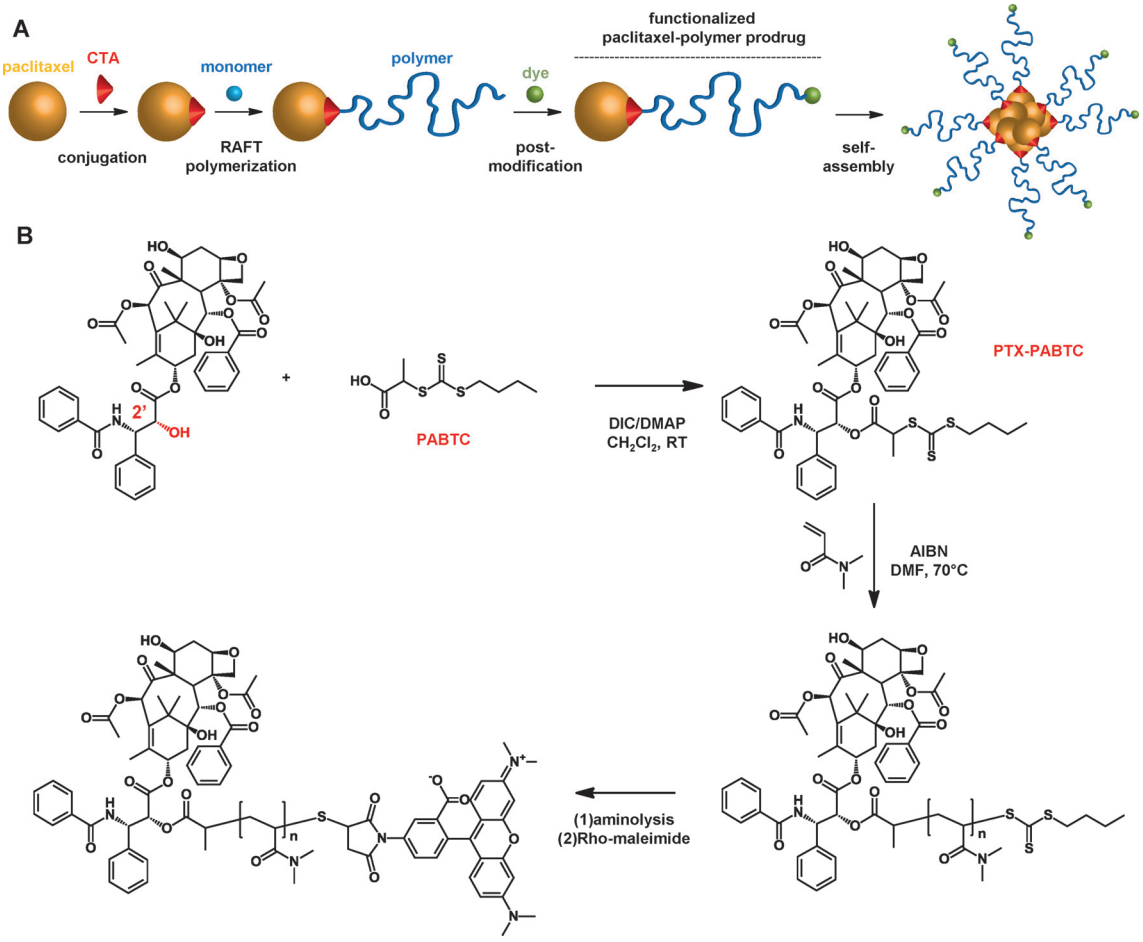

Scheme 1. A) Illustration of the functionalized PTX–polymer prodrug design and (concentration-dependent) self-assembly into nanoparticles in aqueous media. B) Corresponding reaction scheme. Esterification of PTX with a RAFT CTA is followed by polymerization of *N*,*N*-dimethylacrylamide and post-polymerization modification of the trithiocarbonate end group with a maleimide-functional fluorescent dye.

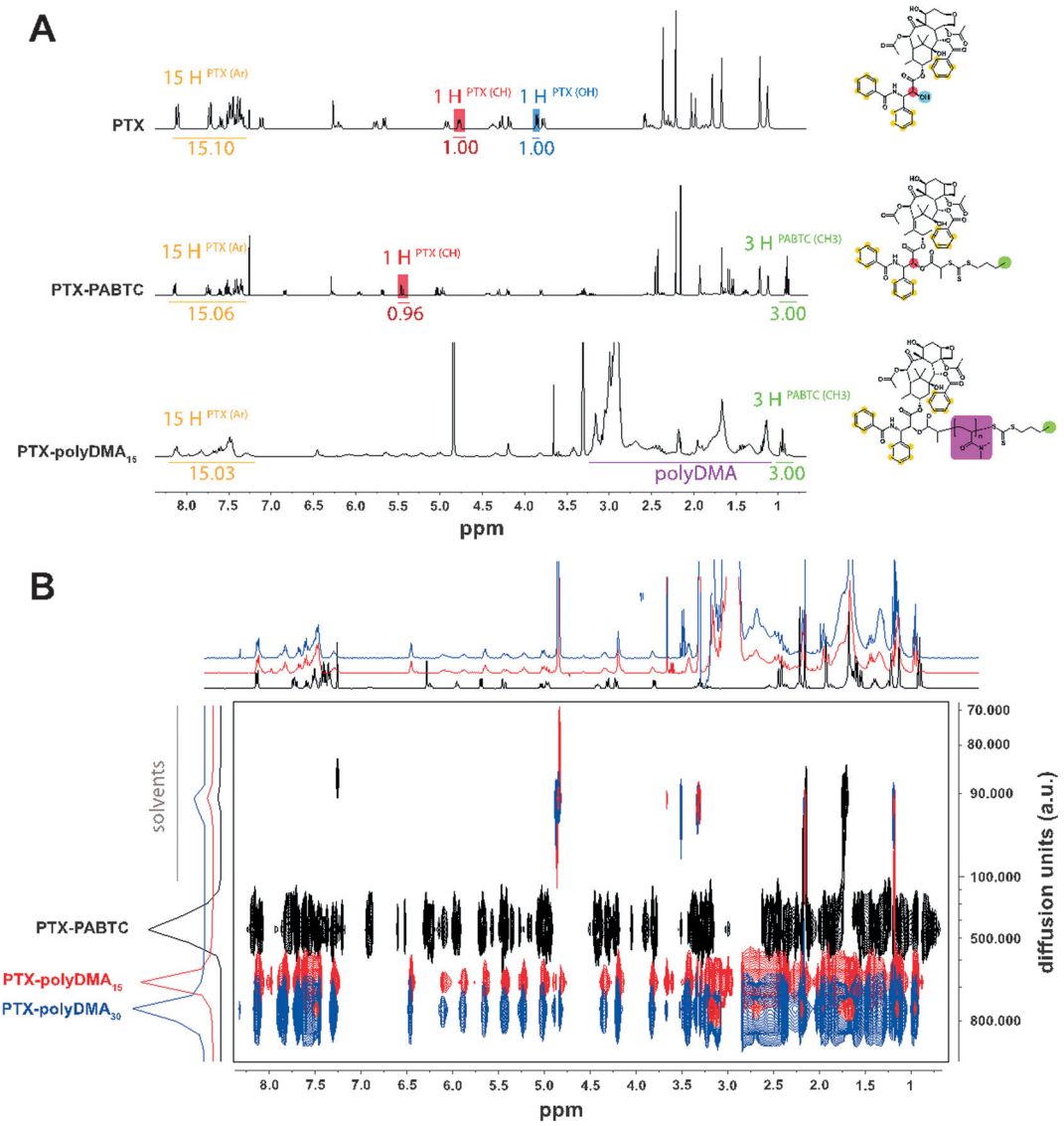

Figure 1. A) ^{1}H and B) DOSY NMR spectra of PTX, PTX–PABTC, and PTX–polyDMA$_{15/30}$.

distribution with no significant low- or high-molecular-weight side products. ^{1}H NMR analysis (Figure 1 A and Figures S17–S20) confirmed the high chain-end fidelity through the excellent agreement between the proton resonances from PTX and PATBC. The absence of free PTX and PTX–PABTC was further confirmed by DOSY NMR spectroscopy (Figure 1 B); these spectra contained polyDMA and PTX resonances for both PTX–polyDMA$_{15}$ and PTX–polyDMA$_{30}$ exhibiting similar diffusional behavior, yet those of higher DP were of slower diffusion. Table 1 summarizes the properties of all polymers after purification.

Next, we investigated the behavior of the PTX–polymer conjugates in aqueous medium. PTX–polyDMA$_{30}$ afforded a transparent formulation, both in H_2O and PBS buffer at concentrations up to at least 30 mg mL^{-1}. At a drug loading of around 21 %, the PTX solubility in aqueous medium was thus increased by more than a factor of 2×10^{4}.[25] By contrast, the PTX–polymer conjugate with a DP of 15 (PTX–polyDMA$_{15}$) could not be solubilized or properly dispersed in aqueous medium (e.g., PBS), even after extensive sonication or decreasing the concentration. This highlights the effect of the hydrophilic-polymer chain length on the resulting solution behavior, but also opens avenues to prepare solid hydrophobic nanoparticles, for example, by solvent displacement in surfactant solution. We subsequently characterized the supramolecular behavior of PTX–polyDMA$_{30}$ in aqueous medium. At a concentration of 30 mg mL^{-1} in PBS, dynamic light scattering (DLS; Figure 2 C) indicated the presence of self-assembled nanostructures, with a *Z*-average hydrodynamic diameter of 27.9 ± 0.8 nm and a narrow dispersity (PDI) of 0.100 ± 0.038 (Figure 2 D). The control polymer polyDMA$_{30}$ formed soluble unimers in PBS at the same concentration (30 mg mL^{-1}). Importantly, over a time course of at least five days, neither a change in size or PDI nor crystallization of released PTX was observed in PBS. These findings highlight the potential of this strategy to obtain stable aqueous PTX formulations that do not suffer from burst drug release. The critical aggregation concentration (CAC) of

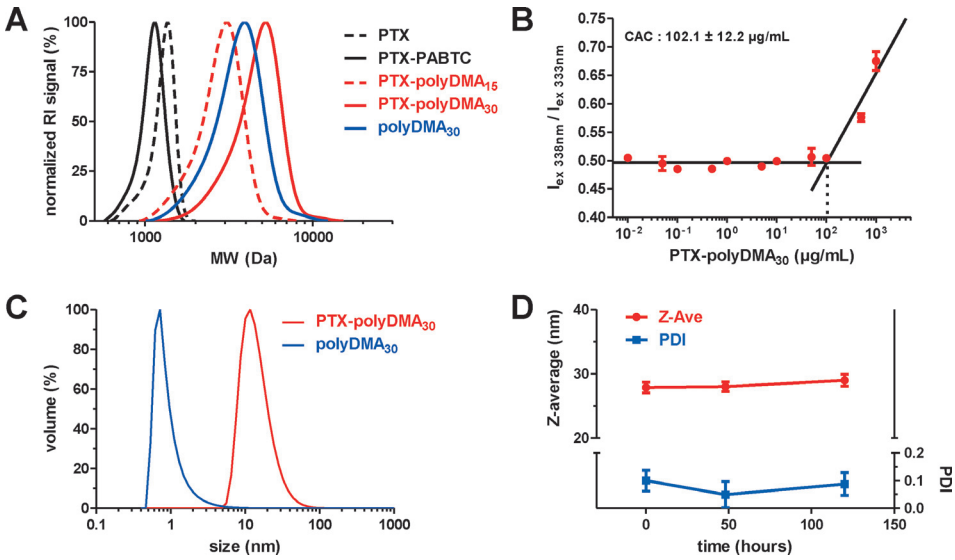

Figure 2. A) SEC elugrams of PTX, PTX–PABTC, PTX–polyDMA$_{15/30}$, and polyDMA$_{30}$. B) CAC of PTX–polyDMA$_{30}$ in PBS determined by a pyrene assay ($n=2$). C) Size distributions of PTX–polyDMA$_{30}$ and polyDMA$_{30}$ (30 mg mL^{-1} in PBS) determined by DLS ($n=4$). D) Colloidal stability of PTX–polyDMA$_{30}$ determined by DLS (30 mg mL^{-1} in PBS, 37 °C; $n=4$).

PTX–polyDMA$_{30}$ was determined by fluorescence spectrophotometry (Figure 2B; pyrene assay) to be 102 ± 12 µg mL^{-1}. This is relatively high compared to typical amphiphilic block copolymers and can be explained by the relative small hydrophobic part of the PTX–polyDMA$_{30}$ conjugate.

The CAC value implies that under physiological conditions, the polymers will likely be present as soluble unimers and are also likely to bind serum proteins. However, if a stable nanoparticulate formulation is desired, the versatility of RAFT polymerization also offers the possibility to introduce reactive co-monomers that could be used for cross-linking or to use degradable monomers with transient solubility.[19]

As mentioned earlier, one of the major advantages of RAFT over other polymerization techniques is the direct access towards α,ω-telechelic polymers.[26] PTX–polyDMA$_{30}$ contains PTX at the α-end, thereby offering an opportunity for post-polymerization modification of the ω-end group,[27] which was demonstrated by attachment of the fluorescent dye tetramethylrhodamine maleimide. First, the trithiocarbonate moiety at the ω-end was converted into a thiol by aminolysis (confirmed by UV/Vis spectroscopy, see Figure S21) and subsequently reacted with tetramethylrhodamine (Rho) maleimide to form a stable thioether bond between polymer and dye. A similar strategy could also be used to introduce radiotracers or targeting ligands. After dialysis, the absence of free dye was confirmed by reverse-phase TLC (Figure S22). DLS further confirmed that conjugation of the rhodamine dye did not significantly alter the supramolecular behavior of the conjugate PTX–polyDMA$_{30}$–Rho (Figure S23).

Subsequently, we evaluated the in vitro behavior of the PTX–polyDMA$_{30}$–Rho conjugate in SKOV-3 human ovarian cancer cells. After two hours of incubation, the intracellular localization of PTX–polyDMA$_{30}$–Rho was investigated by confocal microscopy. As shown in Figure 3A1, a punctuated fluorescence pattern was observed inside the cells, which confirmed that the polymeric prodrug had been efficiently internalized. To shed light on the uptake mechanism, PTX–polyDMA$_{30}$–Rho was co-incubated with Alexa Fluor 488 (AF488) labeled dextran (Figure 3A2) or counterstained with LysoTracker (Figure 3A3). Dextran conjugates are known to be taken up by pinocytosis,[28] thereby staining endosomes, whereas Lysotracker stains lysosomal vesicles. The strong co-localization of PTX–polyDMA$_{30}$–Rho with Dextran–AF488 and the partial co-localization with LysoTracker indicates active endocytosis into intracellular acidic vesicles. When the experiment was repeated at 4 °C, where energy-dependent endocytosis is blocked, no uptake of the conjugate was observed (data not shown). These findings show that in contrast to PTX, which is a membrane-permeable molecule,[29] the polymeric prodrug is actively taken up by endocytosis (e.g., pinocytosis) but not yet abundantly present in lysosomal vesicles within two hours. As PTX is known to exit cancer cells through P-glycoprotein efflux, altering the route through which PTX enters the cell might prolong its intracellular residence and might hold potential for overcoming multidrug resistance.[30]

Next, the effect of PTX–polyDMA$_{30}$ on the in vitro viability of SKOV-3 cells was investigated. Cells were incubated with PTX–polyDMA$_{30}$, the polyDMA$_{30}$ control

Table 1: Compositional data of the synthesized polymers.

Polymer	$[DMA]_0/[CTA]$	DMA conv. [%][a]	DP^{conv} [b]	DP$^{end\ group}$ [c]	M_n [Da][d]	Đ[d]	PTX loading capacity [%][e]
PTX–polyDMA$_{15}$	15	90	14	16	2648	1.09	35
PTX–polyDMA$_{30}$	30	99	30	31	4356	1.07	21
polyDMA$_{30}$	30	91	27	29	3477	1.09	-

[a] Determined by ^{1}H NMR spectroscopy. [b] Determined by ^{1}H NMR spectroscopy, based on monomer conversion. [c] Determined by ^{1}H NMR spectroscopy, based on end group analysis. [d] Analyzed by SEC in DMA, calibrated with PMMA standards. [e] Calculated based on the conversion by ^{1}H NMR spectroscopy: $MW_{PTX}/MW_{PTX-polyDMA} \times 100\%$.

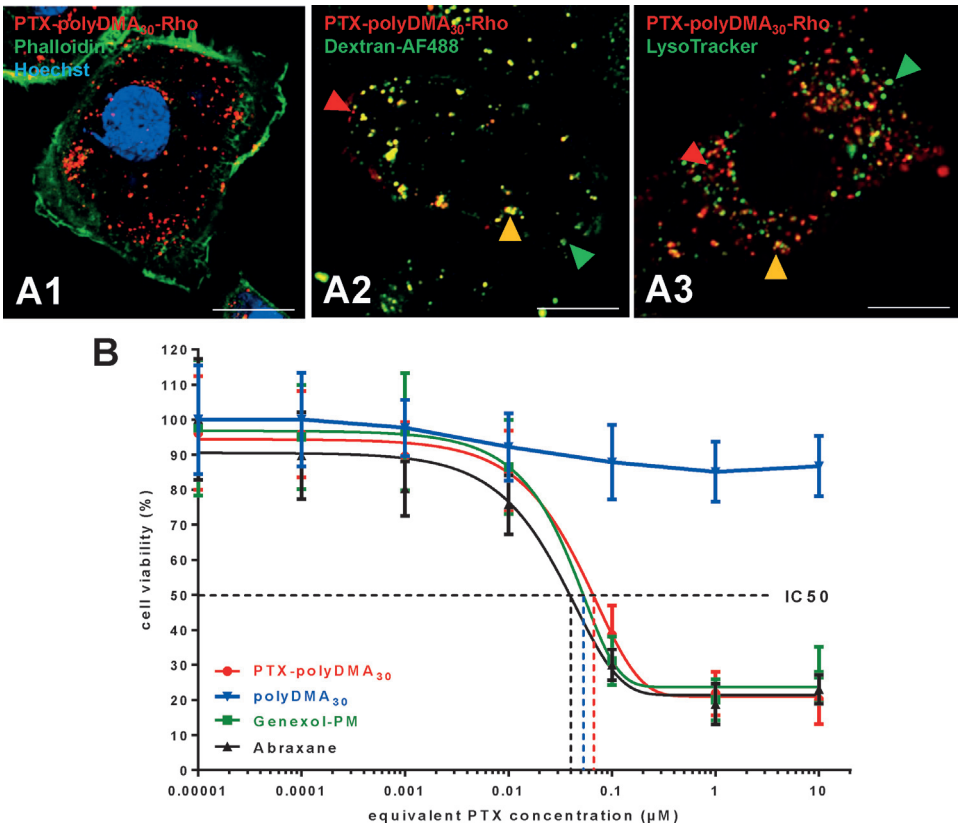

Figure 3. A) Confocal microscopy images of SKOV-3 human ovarian cancer cells incubated with the PTX–polyDMA$_{30}$–Rho conjugate. Counterstaining was performed with Hoechst and Phalloidin to stain cell nuclei and plasma membranes, respectively (A1). The conjugate was co-incubated with Dextran–AF488 to stain (early) endosomes (A2). Lysosomal vesicles were stained with LysoTracker (A3). For guidance, in panels A2 and A3, a co-localization event is marked with a yellow arrow, and two non-co-localization events are marked with red and green arrows, respectively. Scale bars (white, bottom right in each panel) correspond to a length of 15 μm. B) In vitro cytotoxicity of PTX–polyDMA$_{30}$ versus the commercial PTX nanoformulations Abraxane and Genexol-PM. Non-PTX-conjugated polyDMA$_{30}$ was used as a control ($n = 6$).

polymer, and two commercial PTX nanoformulations, Abraxane and Genexol-PM, for 72 h. The cell viability was assessed by an MTT assay. As shown in Figure 3B, no cytotoxicity was observed for the control polymer polyDMA$_{30}$, suggesting that polyDMA is cytocompatible within the experimental window. Interestingly, PTX–polyDMA$_{30}$ exhibited an IC_{50} value of 79 ± 7 nM, which is comparable to those of Abraxane and Genexol-PM (IC_{50} values of 56 ± 11 nM and 65 ± 13 nM, respectively). These findings demonstrate that despite covalent polymer ligation to a position on PTX that is crucial for its bioactivity (the C2′ hydroxy group), the in vitro cytotoxicity effects are similar to those of formulations that rely on mere physical encapsulation. In other words, upon storage in endosomal/lysosomal vesicles, where esterases such as cathepsin B[31] are present, native PTX is released from an inactive polymeric prodrug and can subsequently still reach its subcellular target and exert its cytotoxic activity.

In summary, we have described the synthesis of well-defined polymeric prodrugs of the anticancer drug PTX by a grafting-from-drug RAFT approach. PolyDMA was grown from a regioselectively modified PTX–ester CTA, which resulted in a dramatic increase in the water solubility of the drug upon formation of stable nanoparticles or unimers depending on the concentration. Furthermore, the introduction of a fluorophore at the ω-end of the polymer chain by post-polymerization modification allowed for tracking the intracellular fate of the prodrug. Importantly, the PTX–polymer conjugate showed no loss in in vitro activity.

We believe that the attractiveness of our approach lies in its versatility as it allows for the synthesis of a library of polymer–PTX conjugates starting from a single well-characterized PTX–CTA. Such libraries could encompass different polymer chain lengths, monomers, and side chain or end group functionalities, and could be used to investigate structure–property relationships to alter the pharmacokinetic profile of PTX towards optimal tumor targeting. Furthermore, as the PTX–polymer conjugate is an inactive prodrug, our strategy also holds promise to enhance the maximum tolerable dose (MTD) and thus further improve the therapeutic effect by increasing the administered dose. These investigations, along with studies on active targeting strategies, the use of transiently soluble monomers, and assessing the potential to overcome multidrug resistance, are currently ongoing.

Acknowledgements

B.L., N.V.P., and R.D.C. thank the IWT Flanders and Ghent University (BOF), respectively, for scholarships. B.G.D.G. acknowledges the FWO Flanders and the Flemish Liga Against Cancer for funding. L.N. thanks the Alexander von Humboldt Foundation for a Feodor Lynen fellowship.

Keywords: cancer · nanotechnology · paclitaxel · prodrugs · RAFT polymerization

How to cite: *Angew. Chem. Int. Ed.* **2016**, *55*, 11791–11796
Angew. Chem. **2016**, *128*, 11967–11973

[1] A. F. Wahl, K. L. Donaldson, C. Fairchild, F. Y. F. Lee, S. A. Foster, G. W. Demers, D. A. Galloway, *Nat. Med.* **1996**, *2*, 72–79.

[2] A. Z. Wang, R. Langer, O. C. Farokhzad in *Annu. Rev. Med.*, Vol. 63 (Eds.: C. T. Caskey, C. P. Austin, J. A. Hoxie), **2012**, pp. 185 – 198.
[3] M. Elsabahy, K. L. Wooley, *Chem. Soc. Rev.* **2012**, *41*, 2545 – 2561.
[4] S. Kasmi, B. Louage, L. Nuhn, A. Van Driessche, J. Van Deun, I. Karalic, M. D. P. Risseeuw, S. Van Calenbergh, R. Hoogenboom, R. De Rycke et al., *Biomacromolecules* **2016**, *17*, 119 – 127.
[5] B. Louage, Q. Zhang, N. Vanparijs, L. Voorhaar, S. Vande Casteele, Y. Shi, W. E. Hennink, J. Van Bocxlaer, R. Hoogenboom, B. G. De Geest, *Biomacromolecules* **2015**, *16*, 336 – 350.
[6] N. Desai, *Clin. Cancer Res.* **2006**, *12*, 1317 – 1324.
[7] T.-Y. Kim, *Clin. Cancer Res.* **2004**, *10*, 3708 – 3716.
[8] Y. Shi, R. van der Meel, B. Theek, E. O. Blenke, E. H. E. Pieters, M. H. A. M. Fens, J. Ehling, R. M. Schiffelers, G. Storm, C. F. van Nostrum et al., *ACS Nano* **2015**, *9*, 3740 – 3752.
[9] H. Chen, S. Kim, L. Li, S. Wang, K. Park, J.-X. Cheng, *Proc. Natl. Acad. Sci. USA* **2008**, *105*, 6596 – 6601.
[10] N. Larson, H. Ghandehari, *Chem. Mater.* **2012**, *24*, 840 – 853.
[11] F. Greco, M. J. Vicent, *Adv. Drug Delivery Rev.* **2009**, *61*, 1203 – 1213.
[12] E. M. Pelegri-O'Day, E.-W. Lin, H. D. Maynard, *J. Am. Chem. Soc.* **2014**, *136*, 14323 – 14332.
[13] N. Vanparijs, S. Maji, B. Louage, L. Voorhaar, D. Laplace, Q. Zhang, Y. Shi, W. E. Hennink, R. Hoogenboom, B. G. De Geest, *Polym. Chem.* **2015**, *6*, 5602 – 5614.
[14] K. L. Heredia, D. Bontempo, T. Ly, J. T. Byers, S. Halstenberg, H. D. Maynard, *J. Am. Chem. Soc.* **2005**, *127*, 16955 – 16960.
[15] B. S. Sumerlin, *ACS Macro Lett.* **2012**, *1*, 141 – 145.
[16] P. De, M. Li, S. R. Gondi, B. S. Sumerlin, *J. Am. Chem. Soc.* **2008**, *130*, 11288 – 11289.
[17] J. Xu, K. Jung, N. A. Corrigan, C. Boyer, *Chem. Sci.* **2014**, *5*, 3568.
[18] Q. Zhang, M. Li, C. Zhu, G. Nurumbetov, Z. Li, P. Wilson, K. Kempe, D. M. Haddleton, *J. Am. Chem. Soc.* **2015**, *137*, 9344 – 9353.
[19] N. Vanparijs, R. De Coen, D. Laplace, B. Louage, S. Maji, L. Lybaert, R. Hoogenboom, B. G. De Geest, *Chem. Commun.* **2015**, *51*, 13972 – 13975.
[20] R. Tong, J. Cheng, *Angew. Chem. Int. Ed.* **2008**, *47*, 4830 – 4834; *Angew. Chem.* **2008**, *120*, 4908 – 4912.
[21] D. T. Bui, A. Maksimenko, D. Desmaële, S. Harrisson, C. Vauthier, P. Couvreur, J. Nicolas, *Biomacromolecules* **2013**, *14*, 2837 – 2847.
[22] H. M. Deutsch, J. A. Glinski, M. Hernandez, R. D. Haugwitz, V. L. Narayanan, M. Suffness, L. H. Zalkow, *J. Med. Chem.* **1989**, *32*, 788 – 792.
[23] D. G. I. Kingston, *Chem. Commun.* **2001**, 867 – 880.
[24] P. H. Kierstead, H. Okochi, V. J. Venditto, T. C. Chuong, S. Kivimae, J. M. J. Fréchet, F. C. Szoka, *J. Controlled Release* **2015**, *213*, 1 – 9.
[25] Y. Shi, M. J. van Steenbergen, E. A. Teunissen, L. Novo, S. Gradmann, M. Baldus, C. F. van Nostrum, W. E. Hennink, *Biomacromolecules* **2013**, *14*, 1826 – 1837.
[26] C. Boyer, V. Bulmus, T. P. Davis, V. Ladmiral, J. Q. Liu, S. Perrier, *Chem. Rev.* **2009**, *109*, 5402 – 5436.
[27] H. Willcock, R. K. O'Reilly, *Polym. Chem.* **2010**, *1*, 149 – 157.
[28] E. L. Racoosin, *J. Cell Biol.* **1993**, *121*, 1011 – 1020.
[29] C. Ryppa, H. Mann-Steinberg, M. L. Biniossek, R. Satchi-Fainaro, F. Kratz, *Int. J. Pharm.* **2009**, *368*, 89 – 97.
[30] M. M. Gottesman, T. Fojo, S. E. Bates, *Nat. Rev. Cancer* **2002**, *2*, 48 – 58.
[31] A. Eldar-Boock, K. Miller, J. Sanchis, R. Lupu, M. J. Vicent, R. Satchi-Fainaro, *Biomaterials* **2011**, *32*, 3862 – 3874.
[32] C. J. Ferguson, R. J. Hughes, D. Nguyen, B. T. T. Pham, R. G. Gilbert, A. K. Serelis, C. H. Such, B. S. Hawkett, *Macromolecules* **2005**, *38*, 2191 – 2204.

Received: June 17, 2016
Revised: July 14, 2016
Published online: August 25, 2016

